Mind the gap: Congruence between present and future motivational states shapes prospective decisions

Roni Setton[1], **Geoffrey Fisher**[2], **R. Nathan Spreng**[1]

[1]McGill University, Montreal, QC, Canada, H2X 2C4

[2]Cornell University, Ithaca, NY, USA, 14850

Abstract

Poor estimation of one's future actions has been associated with the influence of reward over executive control processes during prospection. However, the neural mechanisms underlying this reward-control trade-off remain poorly understood. In the present study, we take advantage of projection bias, underestimating how motivations will change in the future, to examine brain and behavior changes during prospection about future decisions. To manipulate motivation, we altered satiety (hungry vs. satiated) and asked human participants (N=25) to place bids on snack foods while undergoing fMRI scanning across two sessions. While hungry, participants bid for the right to consume snacks in both a future congruent motivational state (hungry) and a future incongruent motivational state (satiated). In a second session, while satiated, participants placed bids for the right to immediately consume the items. Imagination of a congruent future state was associated with brain activity in regions implicated in prospection. Imagination of an incongruent future state was related to brain activity in areas related to cognitive control. Projection bias, the difference between bids during incongruent prospection (hungry to satiated, session one) and realization (satiated, session two), was negatively related to thalamic and insular engagement, areas associated with executive control and salience processing. Bias was positively related to engagement of the ventral striatum, a region involved in reward processing. These results suggest that the relative activation between reward and control systems is influenced by the congruence of present and future motivational states, and shapes bias in predictions about future behavior.

Keywords

prospection; decision-making; projection bias

Conflict of Interest: The authors declare no conflict of interest.

1. Introduction

We often make inaccurate predictions about our future behavior. For example, hungry individuals incorrectly predict which food they will want to consume in a future satiated state (Read & van Leeuwen, 1998). This prediction error, known as projection bias, suggests that while people generally understand how their behavior will change in a different context, they fail to anticipate the extent of that change (Loewenstein et al., 2003). The discrepancy between prediction and outcome is in part attributable to contextual differences that evolve along the path from the present to the future (Gilbert & Wilson, 2007). Individuals often rely on their feeling states now to inform predictions about feeling states later and only then make adjustments for the time difference (Gilbert, 2006). Changing contexts may enhance the discrepancy by demanding additional adjustment. Contextual differences may also be altogether disregarded. Despite substantial differences in decision-making contexts, individuals frequently rely on reward associations from past experiences to bias current decisions (Duncan & Shohamy, 2016). Here we leverage projection bias to examine how congruence between present and future motivational states influences prospective decision-making and identify brain regions associated with these changes.

Episodic future thinking (Atance & O'Neill, 2001), or detailed imagining of one's future self, allows one to mentally "try out" different ways in which upcoming events might unfold (cf. Jing et al., 2017; Schacter, 2012). Mounting evidence suggests that vivid episodic future thinking can enhance decisions about the future by attenuating impulsivity, leading to more adaptive, goal-directed responding (e.g., Andrews-Hanna et al., 2014). The constructive episodic simulation hypothesis posits that individuals integrate aspects of past experience to form priors about relevant future experiences (e.g., Schacter & Addis, 2009). Because these priors minimize the psychological distance between present and future selves (Trope & Lieberman, 2010), episodic future thinking and associated engagement of default network brain regions (Addis and Schacter, 2012), should contribute to more accurate depictions of how individuals will act in the future. However, motivational state changes, wherein current reward associations may no longer be relevant to future contexts, may reduce the accuracy of prospective decisions.

Prior work suggests that goal-directed decision-making is supported by engagement of regions related to reward sensitivity and executive control. Ventral striatum, ventromedial prefrontal cortex, and posterior cingulate cortex are associated with subjective value during a variety of decision-making tasks (Clithero & Rangel, 2013). The dorsolateral prefrontal cortex (DLPFC) is associated with executive control processes and is posited to interact with reward-sensitive regions to shape the value of rewards (e.g., Staudinger et al., 2011). DLPFC has also been linked to behavioral restraint towards valued food items while dieting (Hare et al., 2009) and craving suppression for desirable foods while hungry (Hutcherson et al., 2012). Brain regions participating in the processing and top-down control of rewards may therefore work together to adjust behavior during shifting reward contingencies (Samanez-Larkin and Knutson, 2015), but little is known about how they impact prospection for future events.

To investigate the influence of motivational context on brain activity during prospective decision-making, we conducted a fMRI study involving future valuation and projection bias. We examined valuation of food items in conditions of hunger and satiation during fMRI scanning, recognizing that hunger serves as a familiar and powerful manipulation of motivational states (Burnett et al., 2016). First, hungry participants imagined a future state in which they were hungry (congruent) or satiated (incongruent) and placed incentive-compatible bids over a variety of snack items in each scenario. We then measured projection bias by having participants return for a second session of the fMRI task while satiated.

We hypothesized that imagining a congruent future state would recruit brain areas associated with vivid prospection since the psychological distance between the present and future would be at a minimum (e.g, D'Argembeau & Linden, 2004). Conversely, we predicted that imagining an incongruent future state would activate areas related to executive control and reward modulation. Critically, we hypothesized that greater engagement of regions within the default and/or executive control networks, would be associated with lower projection bias, or greater accuracy during prediction of an incongruent future state. That is, perhaps individuals who are more successful at simulating the future or modulating reward are less susceptible to bias. In contrast, we predicted that greater activity in regions that process reward salience would be related to higher projection bias, or lower prediction accuracy. If confirmed, these findings would illuminate the roles of brain regions involved in reward processing, executive control, and the default network during prospective decision-making. These data would also provide evidence that congruence between present and future contexts, i.e., motivational states, is associated with more accurate prospection about one's future behavior.

2. Materials and Methods

2.1. Participants

Twenty-five participants (15 female, 10 male) were scanned twice over two sessions on separate days. Five additional participants were excluded from analysis: three dropped out after the first session, one dropped out in the middle of the first session, and a software problem precluded response recording during the second session for one participant. Participants were recruited through the Laboratory for Experimental Economics and Decision Research sign-up system and the Cornell Magnetic Resonance Imaging Facility. All participants were right-handed young adults between the ages of 18 and 30 years old (M=22.52, SD=2.79) with normal or corrected-to-normal vision. Participants were screened for current use of psychotropic medication in addition to the following criteria: willing to fast for five hours, enjoyed eating snack foods, and had no dietary allergies or restrictions. Participants were compensated with $30 after the first session and $30 after the second session for a total of $60. The study was approved by and carried out in accordance with the Cornell University Institutional Review Board.

2.2. Stimuli

One set of ninety snack items and a separate set of ten snack items (Hare et al., 2011) were used in the present study. Both sets included pictures of fruits and vegetables, chips, candy,

and other assorted snack foods. All items were presented in color on a black background and pictures lacking food packaging were labeled in white text on top of the image. The set of 10 items was presented as part of a practice task on a laptop screen prescan. During scanning, stimuli were reflected from a monitor on a mirror-mounted system in the scanner bay. MRI-safe corrective lenses were used when needed. The Psychophysics Toolbox (Brainard, 1997; Pelli, 1997; Kleiner et al., 2007) implemented in Matlab was used to present stimuli and record responses.

2.3. Procedure

The experiment consisted of two sessions that took place 1 to 7 days apart at the same time each day (*M*=3.16 days, *SD*=1.86 days). Participants arrived to the first session in a fasted state and to the second session in a satiated state. We chose to focus on one direction of contextual changes (hungry to satiated) since our hypotheses were better informed by the well-documented motivational control of behavior by food in humans. The timeline and activities for each session are represented in Figure 1A and described below.

2.3.1.   Session 1.—On the first day, participants were asked to refrain from eating or drinking anything but water for five hours before the start of the experiment (e.g., Plassman et al., 2007; Hare et al., 2011; Hutcherson et al., 2012). To confirm that they followed instructions, participants were asked when they last ate food and what they last ate. They were also asked to use a 7-point Likert scale to answer the questions "How hungry are you right now?" and "How hungry are you normally at this time of day?" where 1 indicated not at all hungry and 7 indicated very hungry. Participants were given detailed instructions about the scanner task and completed a practice task as many times as needed before the scan.

Participants bid on snack food items in two conditions during the scan, both of which involved imagining future scenarios: "Imagine Hungry," where participants placed bids on items imagining that they would return to the second session hungry (after fasting for five hours) and could consume that item after the second session, and "Imagine Satiated," where participants placed bids while imagining a similar scenario, but while satiated (after a full meal). Participants were well informed about the precise meaning of each condition during training. Each trial was considered independent of the others. To encourage participants to bid as closely as they would in real life (and prevent an experimenter demand effect), they were told that one trial from both experimental sessions would be chosen at random and implemented according to a Becker-DeGroot-Marschak (BDM) auction rule (Becker et al., 1964) at the end of the second session (see below for details). Participants were instructed that they would have to remain in the laboratory for an additional 20 minutes after the BDM auction regardless of whether or not the trial chosen resulted in the receipt of a snack. Critically, participants were not informed about whether they would return hungry or satiated for the second session until all activities from the first session were completed to prevent them from biasing their bids.

The bidding task was divided into three 10-minute runs of six blocks for a total of 18 blocks, 9 per condition. Each block began with a cue for the condition that the participant should imagine ("You will be HUNGRY", "You will be FULL"), and commenced with 10 trials in

which bids of $0, $1, $2, or $3 could be placed on each snack item (Figure 1B, left panel). The trial proceeded once the participant responded or after 4 seconds. Confirmation of the bid or "No Response" was presented for 1 second before a fixation cross appeared to mark the start of the next trial. Importantly, faster responses did not speed the task. Any remaining time from the trial was added onto fixation immediately following feedback. Trials were jittered by an inter-trial interval of 1 to 3 seconds. The same 90 food items were shown for each condition and randomized for each participant. Block order was also randomized but constrained to having no more than two of the same condition back-to-back. The scanning session concluded with a fourth 10-minute run where participants saw a black screen and were instructed to rest with their eyes open.

After the scanning session, participants were asked to rate the same snack foods on how much they liked the foods in general using a scale of −3 to 3, where −3 indicated "I really don't like this food" and 3 indicated "I really like this food." Stimulus presentation was randomized and each item appeared only once. Participants were then paid and given instructions for the second session.

2.3.2.   Session 2.—All participants were asked to return to the second session satiated, having eaten a full meal with dessert 30 minutes prior to the start of the session. As on the first day, participants were asked when and what they last ate, as well as how hungry they were, using a 7-point Likert scale (1 = not at all hungry, 7 = very hungry). The scanning session on the second day consisted of a simplified version of the bidding task from the first session (Figure 1B, right panel). During two six-minute runs comprised of 45 trials per run, each of the 90 snack items was shown again and participants could place bids of either $0, $1, $2, or $3 on how much they wanted the food immediately following the end of the session ("Actually Satiated"). This time, each run began with a cue to remind participants of instructions. All other task parameters were equivalent to the scan from the first session. Participants were reminded that one trial from both sessions would be chosen at random and to bid as they would in real life.

After the scan, the liking task was completed a second time as described above. A program then randomly chose one of the trials from both sessions and that trial was implemented according to a BDM auction rule (Becker et al., 1964). In short, the participant's bid was compared to the price of the item in the trial chosen, which was determined by a virtual ball drawn from an urn containing four balls: $0, $1, $2, and $3. If the bid exceeded the price of the item, the participant used his or her earnings from the experiment to pay the price on the ball for the item and received that item. If the bid was equal to or less than the price of the item, he or she did not get the snack at the end of the session and paid nothing. This structure ensured that the bidding mechanism was incentive-compatible. Participants then remained in the laboratory for an additional 20 minutes, as previously instructed, and received their compensation for the second day.

2.4.   Analysis

Repeated measures analyses of variance (ANOVA) were conducted on bidding behavior and response time (RT) to observe whether there were differences across conditions. One

participant was excluded from all RT analyses due to a faulty button on the button box during the second session (all "No Response" bids for that session were replaced with "$1" based on the participant's feedback after the session). No participants were excluded for too many "No Response" trials, but one participant had a notably higher number than the rest (M = 3.52, SD = 9.03, Median = 1). Post-hoc Tukey HSD tests were carried out with an alpha-level of .05, corrected for multiple comparisons, to examine simple main effects. A measure of projection bias was subsequently created by subtracting the mean bid in Actually Satiated from the mean bid in Imagine Satiated for each subject.

2.4.1.   fMRI Data Acquisition and Preprocessing.—All images were acquired with a GE Discovery MR750 3T scanner (General Electric, Milwaukee, United States) with a 32-channel receive-only phased-array head coil at the Cornell Magnetic Resonance Imaging Facility in Ithaca, New York. Anatomical scans were acquired with Tl-weighted volumetric MRI magnetization prepared rapid gradient echo and sensitivity encoding (TR=2530ms; TE=3.42ms; TI= 1100ms; Flip Angle (FA)=7°; FOV=256×256mm; sampling bandwidth=25 kHz; voxel size=1mm isotropic; 176 slices; acceleration factor=2; scan time=5:25'). All functional imaging data were acquired using a multi-echo echo planar imaging sequence with online reconstruction and sensitivity encoding (TR=3000ms; TEs= 13.7, 30, 47ms; FA= 83°; matrix size=72 × 72mm; FOV=210mm; voxel size= 3mm isotropic; 46 axial slices; acceleration factor=2.5; scan time=9:51', 6:03', 10:06' for the bidding task during the first and second sessions, and the resting state scans following both sessions). Participants made responses during task runs with a four-button response box held in the right hand.

Task imaging data were preprocessed with Multi-Echo Independent Components Analysis (ME-ICA) version 3 (Kundu et al., 2012; Kundu et al., 2013), which has been implemented in both resting state and task-based MRI (Lombardo et al., 2016; DuPre et al., 2016). Briefly, ME-ICA is a preprocessing pipeline that makes use of the linear TE dependence properties of blood-oxygen-level-dependent (BOLD) signal to better distinguish between signal and non-neural sources of noise such as physiologic- and motion-derived artifact. The de-noised time series from all three echoes are then optimally combined to maximize the signal-to-noise ratio. Here, anatomical images were first skull stripped using default parameters in FSL BET. ME-ICA processing was then run with the options to remove the first four volumes of data and to warp to MNI space using a high-resolution template (MNI_caez_N27). The optimally-combined de-noised time series were smoothed with a 6mm FWHM kernel in AFNI. Data from resting-state scans were not considered here.

2.4.2.   fMRI Data Analysis.—SPM8 (Wellcome Department of Imaging Neuroscience, Institute of Neurology, London, UK) was used to estimate two event-related general linear models (GLM) with three specific aims: (i) to initially confirm that activity for increasing bids was consistent with previous work on brain regions involved in parametric modulation of subjective value (see Clithero & Rangel, 2013 for a metaanalysis); (ii) to examine how congruent and incongruent future motivational contexts impact brain activity during prospection; (iii) to explore how these changes affect bidding behavior and projection bias.

The first model (GLM1) combined data from both sessions in a single design matrix and was estimated with the following regressors to satisfy aims (i) and (ii): trial onsets for

Imagine Hungry, a parametric modulator for bids in Imagine Hungry, trial onsets for Imagine Satiated, a parametric modulator for bids in Imagine Satiated, trial onsets for Actually Satiated, and a parametric modulator for bids in Actually Satiated. Importantly, parametric modulation made it possible to observe how higher value is represented in a congruent compared to an incongruent context. Additional regressors of no interest included the first trial of each block and trials with no responses. Since the data were de-noised within ME-ICA, no additional noise regressors were included. All regressors were modeled as stick functions with durations of 0. Time and dispersion derivatives were included to allow for variation in the amplitude and width of the hemodynamic response function. A standard 95% probability grey matter mask (MNI152 T1-weighted average structural template) was applied at the subject level for subsequent analyses to ensure that voxels with less than 5% probability of being grey matter were removed.

First-level contrasts were initially created to observe average brain activity during task (All task > 0) and during parametric modulation of bids throughout the task (All bids > 0). Next, we contrasted average activity during congruent prospection (Imagine Hungry) to that during incongruent prospection (Imagine Satiated) and parametric modulation during these conditions (Imagine Hungry bids > Imagine Satiated bids; Imagine Satiated bids > Imagine Hungry bids).

A second general linear model (GLM2) was estimated to explore how imagining a different motivational state affected brain activity associated with projection bias. Specifically, we wanted to observe how brain changes during Imagine Satiated (session 1) versus Actually Satiated (session 2) were associated with projection bias. Doing so required a second GLM since projection bias scores were derived from bids in Imagine Satiated and Actually Satiated, which accounted for some variance GLM1. Like GLM1, GLM2 included all data from both sessions. Trial onsets for all three conditions were entered into an identical fixed effects model as above but without parametric modulation. RT was added as a parametric modulator post-hoc to ensure that brain activity related to projection bias exceeded any behavioral correlation between bids and RT during Imagine Satiated and Actually Satiated. First-level contrasts were created for Imagine Satiated > Actually Satiated and brought to the second level, where we regressed participants' projection bias scores.

An additional post-hoc model (GLM3) was estimated to observe how differences in bid value across conditions affected our main brain results. Significant differences in mean bid amounts across conditions could confound results comparing the modulation of bids between conditions. To ensure that modulation of bids in Imagine Hungry > Imagine Satiated did not merely reflect a difference in mean bids between the conditions, and thus high versus low value, trials with bids of $0 and $1 were entered into a fixed effects model as "low value" while trials with bids of $2 and $3 were entered as "high value" to compare BOLD signal between highly valued items and lesser-valued items in Imagine Hungry alone. First-level contrasts were created for High > Low value and brought to the second level for comparison with the pattern of brain activity observed during parametric modulation of Imagine Hungry > Imagine Satiated.

All first-level contrasts were entered into a random effects model at the second level for whole brain analyses. One-sample t-tests were performed to examine overall group effects. We report results with a threshold of p<.001 and an extent volume of 10 voxels to capture subtle effects within small subcortical structures (unless otherwise noted for more robust effects). Clusters were overlaid with anatomical masks using the Harvard-Oxford atlas in FSLView (Jenkinson et al., 2012) to help with identification. Results were displayed on an inflated surface map (PALS-B12) using Caret software (Van Essen, 2005) or on a T1 MNI template (MNI152_T1_1mm.nii) where appropriate. The seven-network solution by Yeo and colleagues (2011), the result of a clustering algorithm that parcellates cerebral cortex into functionally connected large-scale brain networks based on resting state MRI, was overlaid on volumes in FSLView (Jenkinson et al., 2012) to visually inspect how results clustered along large-scale networks. Scatterplots were created by extracting the beta weights from reported clusters and plotting against behavior for display purposes only.

3. Results

3.1. Behavior

All participants arrived hungry on the first day and satiated on the second day. In addition to subject reports to the experimenter, hunger ratings prior to each scanning session confirmed compliance with task instructions (Session 1: M=5.40, SD=1.19; Session 2: M=1.20, SD=0.82; $t(24)$=14.59, p<.0001, d=2.91).

A repeated measures ANOVA was conducted to assess how mean bid amounts compared across Imagine Hungry, Imagine Satiated, and Actually Satiated. Dots in the left panel of Figure 2A represent the distribution of bids across each condition. Bids were significantly altered by condition ($F(2, 48)$=71.44, p<.0001, η_p^2=0.75; Figure 2A left panel), such that bids for Imagine Hungry (M=$1.43, SD=$1.06) were higher than those for Imagine Satiated (M=$0.93, SD=$0.96), which were in turn higher than those for Actually Satiated (M=$0.60, SD=$0.87; all p<.0001). Results were similar when hunger level (1-7 hunger rating from beginning of each session), gender, body mass index, and days between experimental sessions were included as covariates ($F(2, 47)$=70.57, p<.0001, η_p^2=0.55). A follow-up ANOVA was conducted on the count of trials receiving each bid amount to observe how the occurrence of different bids changed across conditions. A main effect of bid amount ($F(3, 258)$=48.70, p<.001, η_p^2=0.36) was found such that across conditions, bids of $0 ($M$=33.05, SD=24.14) and $1 ($M$=31.65, SD=14.72) were more frequent than bids of $2 ($M$=16.75, SD=12.43) or $3 ($M$=8.03, SD=10.47; all p<.0001). Bids of $2 were also more frequent than $3 ($p$<.05). An interaction effect showed that the pattern of bids was significantly influenced by condition ($F(6, 258)$=18.65, p<.001, η_p^2=0.30; Figure 2A right panel). Tukey contrasts indicated that the frequency of $0 bids increased from Imagine Hungry (M=15.92, SD=12.96) to Imagine Satiated (M=31.48, SD=18.09; p<.001) to Actually Satiated (M=51.76, SD=25.09; p<.0001). Within Imagine Hungry, bids of $1 ($M$=32.56, SD=12.78; all p<.0001) were most prevalent and bids of $2 ($M$=26.64, SD=10.97) were at least trending higher than in any other condition (p=0.06 compared to Imagine Satiated, p<.0001 compared to Actually Satiated). Bids of $0 and $1 ($M$=32.56, SD=12.78) were more popular in Imagine Satiated (all p<.0001), and bids of $0 dominated in Actually Satiated (all p<.0001).

A full listing of pairwise comparisons is provided in Table S1. Results from both ANOVAs on bidding behavior demonstrated that participants understood the *direction* in which their behavior should change when they imagined being satiated (while hungry), but not the *extent* to which it would change when they were actually satiated. These results are consistent with prior observations of projection bias (Read & van Leeuwen, 1998; Loewenstein et al., 2003; Fisher & Rangel, 2014).

Mean bids from Imagine Satiated and Actually Satiated were used to calculate projection bias scores for neuroimaging analyses (M=\$0.32, SD=\$0.31; Figure 2C bottom panel). All scores were within 3 standard deviations of the mean. Bias scores did not differ based on counter-balancing the order of Imagine Satiated and Imagine Hungry in the first session ($t(22.94)$=−1.2905, p=0.21, d=−.49). When projection bias was alternatively calculated at an item level for each participant, all participants exhibited unimodal distributions, confirming that the mean-derived scores accurately reflected bias for each participant. Projection bias scores were not correlated with the change in hunger level ratings from the start of each session ($t(23)$=0.16, p=0.46).

A second repeated measures ANOVA was run to determine whether RT varied with condition, bid amounts, or their interaction. The distribution of RT across each condition is shown in the left panel of Figure 2B. There were main effects of condition ($F(2, 46)$=29.85, p<.0001, η_p^2=0.62; Figure 2B left panel) and bid amount ($F(3, 69)$=20.95, p<.0001, η_p^2=0.51; Figure 2B right panel) on RT, but an interaction effect was only marginal ($F(6, 69)$=2.09, p=.06, η_p^2=0.11). Post-hoc pairwise comparisons of RT between conditions indicated that RT was faster during Actually Satiated (M=1.29s, SD=0.59s) than either Imagine Hungry (M=1.55s, SD=0.69s) or Imagine Satiated (M=1.54s, SD=0.69s; all p<.0001), possibly reflecting practice effects on the task. There was no difference in RT between Imagine Hungry and Imagine Satiated (p=0.92) suggesting that overall processing demands were similar between the two imagination conditions. Post-hoc comparisons of RT between bid amounts demonstrated that RT was faster for bids of \$0 (M=1.32s, SD=60s; all p<.0001) and \$3 (M=1.36s, SD=53s; p<.001 and p<.05 respectively) compared to bids of \$1 (M=1.58s, SD=.63s) and \$2 (M=1.54s, SD=.59s). There was no difference in RT between bids of \$0 and \$3 (p=0.28) or bids of \$1 and \$2 (p=0.87). To further investigate the association between bid amounts and RT, we conducted Spearman correlations across participants for each of the experimental conditions. Bids were positively associated with RT during Imagine Satiated (ρ=.17, p<.0001) and Actually Satiated (ρ=.41, p<.0001). While RT varies for a variety of reasons, one possibility is that bidding higher involved greater deliberation during both the Imagine and Actually Satiated conditions. Results remained similar when hunger level (1-7 hunger rating from beginning of each session), gender, BMI, and days between experimental sessions were included as covariates (Main effect of condition: $F(2, 46)$=29.12, p<.0001, η_p^2=0.62; Main effect of bid: $F(3, 69)$=20.95, p<.0001, η_p^2=0.51; Interaction: $F(6, 69)$=2.09, p=0.06, η_p^2=0.11).

3.2.   Neuroimaging

Our first aim was to ensure that we captured brain activity related to valuation during our bidding task. This was an important initial step since context may directly alter value

representations in the brain. For completeness, we collapsed across conditions to look at both the overall activity during task (All task > 0) and the parametric modulation of bid amounts on food items (All bids > 0) using GLM1. BOLD signal during task (Figure 3A) was observed in large clusters across lateral frontal and parietal regions, cingulate cortex, and medial prefrontal cortex, broadly consistent with the frontoparietal network (Yeo et al., 2011). Large clusters were also observed in thalamus, fusiform gyrus, and occipital cortex (see Table 1 for a full listing). BOLD signal that scaled with higher bids (Figure 3B), and therefore higher subjective value, included smaller clusters in lateral frontal and parietal cortices in addition to larger clusters in orbitofrontal cortex, cingulate cortex, dorsal and ventral striatum, thalamus, and hippocampus (see Table 2 for a full listing). These results are consistent with areas previously associated with subjective value computations (Clithero & Rangel, 2013).

We next compared average activity and parametric modulation during Imagine Hungry and Imagine Satiated to determine how brain activity during imagination is altered by context (congruent versus incongruent future states; GLM1). No clusters passed threshold for average task activity in Imagine Hungry > Imagine Satiated. However, parametric modulation demonstrated that higher bids during Imagine Hungry > Imagine Satiated were associated with greater activity in dorsal striatum, hippocampus, and lateral occipital cortex (Figure 4A–B, see Table 3 for a full listing). The lower bids in Imagine Satiated compared to Imagine Hungry (Figure 2A, left panel) may appear to indicate insufficient power to compare parametric modulation in the two conditions, especially since bids of $0 were more frequent during Imagine Satiated (Figure 2A, right panel). Dots in the left panel of Figure 2A represent means for each participant by condition to illustrate how the data cluster. More concretely, no parametric modulators were dropped for any participants. To further examine whether these results reflected projected values as separable from simply high versus low value, an additional model (GLM3) was estimated for low- and high-valued items in Imagine Hungry alone. Unlike the parametric modulation of bids in Imagine Hungry > Imagine Satiated, group brain activity for High > Low value in Imagine Hungry largely overlapped with regions of the default network and value computation (Figure 4C, see Table 4 for full listing). Lastly, greater task activity was observed during Imagine Satiated > Imagine Hungry in clusters within the precuneus as well as lateral frontal and parietal regions, independent of parametric modulation (Figure 5, see Table 5 for a full listing). Brain activity associated with parametric modulation during Imagine Satiated > Imagine Hungry did not pass threshold.

Our final aim was to explore how brain changes during imagined future episodes involving different motivational contexts impact decision-making behavior. To do this we used our second model without parametric modulation (GLM2) to contrast Imagine Satiated > Actually Satiated. This allowed us to measure BOLD signal unique to prospection of an incongruent state compared to the actual experience of that state. We then regressed behavioral projection bias scores to explore how brain activity during prospection of an incongruent state specifically related to bidding accuracy between imagination and realization. Greater activity in the medial dorsal nucleus of the thalamus (MDNThal) and opercular cortex/posterior insula was related to a smaller difference between Imagine Satiated bids and Actually Satiated bids (Figure 6A–B, Table 6). While the peak of the

MDNThal cluster also bordered on posterior caudate nucleus, functional connectivity and co-activation maps in Neurosynth (Yarkoni et al., 2001) made MDNThal a more likely candidate. Greater activity in the nucleus accumbens was related to a larger difference between bids during Imagine Satiated and Actually Satiated (Figure 6C, Table 6). Because bids were positively correlated with RT during both Imagine Satiated and Actually Satiated conditions, we re-ran GLM2 with RT as a parametric modulator (n=24 due to incomplete RT data from session 2 for one participant). None of the three clusters related to projection bias were correlated with RT (even at an uncorrected threshold of $p < .05$).

4. Discussion

Here we investigated how brain activity during prospection is influenced by motivational context. We examined how imagining a congruent versus an incongruent motivational state influences subjective value and associated brain activation during prospective decision-making. We observed that as participants assigned higher value to food items, they engaged regions associated with reward valuation (Clithero & Rangel, 2013). Our main behavioral results showed that the value prospectively assigned to affectively-valenced items (i.e., food) is shaped by motivational context. During prospection about a congruent motivational state, valuation was linearly associated with the recruitment of subcortical structures that have been related to reward contingencies and prospection. In contrast, imagining an incongruent future context was associated with the recruitment of lateral frontoparietal areas related to cognitive control. Projection bias, a measure of distortion about predicted future behavior, was negatively correlated with activity in MDNThal and opercular cortex/posterior insula, and positively correlated with activity in ventral striatum. These findings suggest that prospection and its underlying brain activity are influenced by the congruence of present and future motivational contexts. Preliminary brain-behavior results demonstrate that regions associated with executive function and reward may determine susceptibility to bias when the future deviates from the present.

4.1. Brain activity during value-based decision-making

We first confirmed that the bidding task engaged regions associated with valuation. We predicted that higher bids placed on food items would reflect higher perceived value for those items, resulting in higher activity in brain regions associated with subjective value (e.g., Clithero & Rangel, 2013). Task activity largely overlapped with the frontoparietal network, consistent with a role for this network in top down attentional control (Vincent et al., 2008). Importantly, activity related to higher bid values engaged ventromedial prefrontal cortex, ventral striatum, and posterior cingulate cortex (Kable & Glimcher, 2007; Levy & Glimcher, 2011; Bartra et al., 2013). These results strongly suggest that our bidding task effectively captured brain activity related to value computation.

4.2. Influence of motivational context on brain activity during future valuation

Our primary aim was to understand how changes to future context impact functional brain activity during prospection. We observed that participants bid higher during congruent prospection than during incongruent prospection, which was associated with greater activity in the caudate nucleus and hippocampus, among other regions. Lateral frontoparietal brain

regions were then engaged more during incongruent prospection relative to congruent prospection.

Co-activation of the caudate and hippocampus for items of increasing value during imagination of an identical future state draws attention to an underrated role for the hippocampus in value-based decision-making. Dopaminergic innervation of the caudate has been linked to reward prediction and anticipation (Schultz, 2000) especially in the context of action-reward contingencies. As part of the default network, the hippocampus has been reliably associated with episodic processes such as declarative memory retrieval and prospection (Buckner et al., 2008). Given that the hippocampus reorganizes its network topology during vivid memory retrieval (Geib et al., 2017), the selective presence of hippocampal activity during imagination of highly valued items in a congruent future context may be related to vivid prospection (e.g., Spreng et al., 2015). Supporting evidence comes from affective forecasting experiments where individuals have been observed to draw on the information they have in the present to make predictions about the future (see Gilbert, 2006 for a review). In fact, current feeling states appear to be an integral part of predicting future feeling states (DeWall & Baumeister, 2006 as in Gilbert, 2006). It is possible that here, too, participants were using their present motivational states to conjure episodic simulations of a similar imagined future. While we cannot be certain that participants were imagining future scenarios during task, we surmise that they were in fact projecting from the visibly distinct clusters present during high- versus low-valued items in the congruent condition alone: a pattern of brain areas similar to those observed as part of the beta valuation system, thought to be sensitive to immediately-available rewards (McClure et al., 2004). It is unlikely that this outcome was impacted by a skew towards bids operationalized as "low value" in Imagine Hungry since each participant had at least 10 trials (and often more) with "high value" bids.

Hippocampal and caudate activity during high-value trials in the congruent compared to the incongruent condition may also emerge due to activation of established reward associations formed in similar real-world contexts. Representations within subregions of the hippocampus have been found to distinguish between low- and highvalued reward items (Wolosin et al., 2013), possibly through dopaminergic associative binding processes (Shohamy & Adcock, 2010). Greater reliance on past rewarding experiences in novel decision contexts has been related to greater connectivity between the hippocampus and caudate nucleus (Wimmer & Shohamy, 2012). In contrast, hippocampal connectivity with medial prefrontal regions has been shown to attenuate the discounting of delayed rewards when participants engage in episodic future thinking (e.g., Peters & Buchel, 2010). The hippocampus may therefore serve as an integral structure in balancing reliance on past and future thought during prospective decisions. Taken together, future motivational contexts similar to the present may invoke strong, highly detailed reward associations that have the propensity to bias behavior to the past via hippocampal and caudate engagement.

We predicted that adjusting behavior during an incongruent future motivational context would require additional cognitive effort to suppress the salience of the current motivational state. Overall, participants were successful in modulating their behavior, as reflected by lower bids in an incongruent future context. This does not reflect a lack of effort or

deliberative processing in Imagine Satiated; when participants bid higher, they took longer to do so. Similarly, there was no evidence for differences in overall processing demands between Imagine Satiated (incongruent) and Imagine Hungry (congruent) based on RT. However, whole-brain results suggest that the nature of the processing differed between these conditions. Several lateral frontal and parietal clusters, implicated in cognitive control, were robustly recruited during an incongruent motivational context. Broadly, prefrontal cortex plays a pivotal role in cognitive control, with the ability to draw on representations of normative behavior during varying task demands and to maintain these representations online as needed (Waskom et al., 2014). Consistent with this idea, DLPFC was recruited when hungry participants were asked to reduce their hunger cravings to desirable foods (Hutcherson et al., 2012) and connectivity between DLPFC and ventromedial prefrontal cortex was increased when highly self-controlled dieters chose healthy foods over non-healthy foods (Hare et al., 2009). The middle frontal gyrus activity observed here may reflect the simultaneous process of drawing on representations of an incongruent state while suppressing the current state in order to lower bid values, but additional data is needed to test this directly. More rostral areas of prefrontal cortex have been associated with simulating future episodes, including intentional aspects of prospective thinking and holding intentions online (Addis et al., 2007; Okuda et al., 1998). Because damage severely impairs prospection (Burgess et al., 2000), rostral prefrontal cortex may be necessary to make predictions about incongruent motivational contexts.

These data suggest that congruence between present and future motivational contexts is a key factor in prospective decision-making. Congruence may provoke episodic future thinking predicated on the present or activate existing, perhaps vivid, reward associations, whereas incongruence necessitates additional resources that are likely involved in executive control to adjust behavior away from the current state. Future work with more data and varying motivational contexts should be carried out to, (i) more precisely examine how hippocampus and caudate cooperate for prospective decisionmaking in congruent contexts and (ii) determine the necessity and sufficiency of prefrontal brain areas for value modulation during prospection in incongruent contexts.

4.3. Brain activity during prospection of an incongruent motivational context related to projection bias

Our final aim was to explore how brain activity during imagination of an incongruent future state may predict behavior during the realization of that state. Lower bids during realization of the incongruent state demonstrated evidence for a projection bias. However, as with Imagine Satiated, here too, participants took longer to respond during higher bids. This suggests that participants remained deliberative during the task, despite a main effect of lower RT in Actually Satiated. While we are unable to definitively resolve lower RT in Actually Satiated in the current study, we speculate that it may be attributable to practice effects since participants previously completed a similar task in session one.

At the level of the brain, we hypothesized that greater accuracy in bids (lower bias) would be associated with greater activity within regions of the default and executive control networks. We reasoned that accurate prediction for how one would behave in an incongruent context,

barring environmental changes beyond one's control, may be attributable to either better episodic future thinking, better cognitive control, or both. We also hypothesized that heightened salience of reward during prospection, demonstrated by greater activation of subcortical regions associated with reward processing (Litt et al., 2011), may interfere with task demands and contribute to lower accuracy (higher bias).

Projection bias scores were negatively correlated with clusters in the MDNThal and operucular cortex/posterior insula. The MDNThal receives input from a number of subcortical areas and acts as a higher order thalamic relay nucleus in learning and decision-making by projecting to prefrontal cortex and posterior insular cortex (Swenson, 2006; Johansen-Berg & Rushworth, 2009). MDNThal has been identified as one of several reliable regions that compute subjective value (Clithero & Rangel, 2013), and humans with damage to the same region demonstrate executive function impairments (Mitchell, 2015). Posterior insula has been shown to play a role in regulation of physiological reactivity and homeostatic activity (Menon & Uddin, 2010). Together these regions may form a cortico-thalamo loop to regulate behavior during incongruent prospection. Specifically, opercular cortex/posterior insula may evaluate the current motivational state, while the MDNThal subsequently integrates information from these (and other lateral control regions engaged during incongruent prospection) to modify behavior. If opercular cortex/posterior insula is pre-occupied with the current motivational state (Loewenstein, 1996; see Reisberg et al., 1989 for other modalities) such that cross talk with MDNThal is obstructed during imagination of an incongruent motivational state, projection bias may transpire. In this way, thalamic and opercular/insular activity may impart a modulatory influence during prospective decision-making to narrow the gap between different present and future contexts.

We observed that activity in the nucleus accumbens was positively correlated with the magnitude of projection bias, consistent with our prediction that higher bias would result from heightened subjective value in subcortical reward-related regions. As part of the ventral striatum, the nucleus accumbens develops early and continues to play a leading role in reward valuation, learning, and expectation throughout the lifespan (Schultz, 2000). Independent of task, the nucleus accumbens is robustly associated with the computation of subjective value (Clithero & Rangel, 2013). Furthermore, Litt and colleagues (2011) observed that the ventral striatum has overlapping representations of value and salience. Within the context of our results, nucleus accumbens activity may reflect a strong preference or motivational incentive salience to eat valuable snack food items during Imagine Satiated due to participants' hungry state. More broadly, the prominence of a current motivational state may disproportionately elevate activity in the nucleus accumbens and reduce the influence of top-down control processes, which may in turn distort behavior during prospection of incongruent motivational contexts.

Additional work is required to interpret these preliminary brain-behavior relationships. Our results provide initial evidence that differential activation of brain regions relate to bias, but we do not suggest that separate neural correlates act in isolation to result in different behaviors. However, corroborating results on the involvement of posterior insula and ventral striatum on pain and market placebo effects (see Plassmann & Weber, 2015 for a review)

suggest to us that somatosensory awareness, executive control, and reward salience all play a role in the motivational signal that precedes bias. More data is needed to further shed light on how biased prediction for incongruent contexts arises in the brain.

5. Conclusions

Here we advance current understanding of the role of episodic future thinking in decision-making by demonstrating the impact of motivational state (congruent versus incongruent) on behavior and functional brain activity during prospection. When a future motivational state was incongruent, the degree of bias in future decision-making was related to the extent of activity in regions associated with executive function versus reward processing. While the magnitude of projection bias has been shown to remain similar in other incongruent motivational contexts (i.e., when satiated participants make predictions about imagined hungry states; Fisher & Rangel, 2014), follow-up studies should probe whether brain mechanisms are also similar. We acknowledge the inextricable link between physiological state and context in this study, but within the broader context of mental time travel, these findings suggest that mental representations of both the past and the future are determined, at least in part, by our present motivational state. Critically, the salience of one's present state may distort prospective decisionmaking when it is incongruent with the future decision-making context. Moreover, further inquiry into the influence of current and imagined future states on reward processing and executive functioning during prospection, and the associated neural mechanisms, will advance our understanding of how we mentally bridge the gap between our current and imagined realities in the service of adaptive, goal-directed behavior.

Supplementary Material

Refer to Web version on PubMed Central for supplementary material.

Acknowledgments

References

Addis DR, & Schacter DL (2012). The hippocampus and imagining the future: Where do we stand? Frontiers in Human Neuroscience, 5(January), 1–15. 10.3389/fnhum.2011.00173

Addis DR, Wong AT, & Schacter DL (2007). Remembering the past and imagining the future: common and distinct neural substrates during event construction and elaboration. Neuropsychologia, 45(7), 1363–1377. [PubMed: 17126370]

Andrews-Hanna JR, Smallwood J, & Spreng RN (2014). The default network and self-generated thought: Component processes, dynamic control, and clinical relevance. Annals of the New York Academy of Sciences, 1316(1), 29–52. 10.1111/nyas.12360 [PubMed: 24502540]

Atance CM, & O'Neill DK (2001). Episodic future thinking. Trends in Cognitive Sciences, 5(12), 533–539. 10.1016/S1364-6613(00)01804-0 [PubMed: 11728911]

Bartra O, McGuire JT, & Kable JW (2013). The valuation system: A coordinate-based meta-analysis of BOLD fMRI experiments examining neural correlates of subjective value. NeuroImage, 76, 412–427. 10.1016/j.neuroimage.2013.02.063 [PubMed: 23507394]

Becker G, DeGroot M, & Marschak J (1964). Measuring utility by a single-response sequential method. Behavioral Science, 9, 226–232. [PubMed: 5888778]

Brainard DH (1997). The psychophysics toolbox, Spatial Vision 10:433–436. [PubMed: 9176952]

Buckner RL, Andrews-Hanna JR, & Schacter DL (2008). The brain's default network: Anatomy, function, and relevance to disease. Annals of the New York Academy of Sciences, 1124, 1–38. 10.1196/annals.1440.011 [PubMed: 18400922]

Burgess PW, Veitch E, de Lacy Costello A, & Shallice T (2000). The cognitive and neuroantomical correlates of multitasking. Neuropsychologia, 38, 10.1016/s0028-3932(99)00134-7

Burnett CJ, Li C, Webber E, Tsaousidou E, Xue SY, Bruning JC, & Krashes MJ (2016). Hunger-driven motivational state competition. Neuron, 92(1), 187–201. 10.1016/j.neuron.2016.08.032 [PubMed: 27693254]

Clithero J. a., & Rangel A (2013). Informatic parcellation of the network involved in the computation of subjective value. Social Cognitive and Affective Neuroscience, 9(9), 1289–1302. 10.1093/scan/nst106 [PubMed: 23887811]

Duncan KD, & Shohamy D (2016). Memory states influence value-based decisions. Journal of Experimental Psychology: General, 145(11), 1420–1426.10.1037/xge0000231 [PubMed: 27797556]

D'Argembeau A, & Van Der Linden M (2004). Phenomenal characteristics associated with projecting oneself back into the past and forward into the future: Influence of valence and temporal distance. Consciousness and Cognition, 13(4), 844–858. 10.1016/i.concog.2004.07.007 [PubMed: 15522635]

DeWall CN, & Baumeister RF (2006). Alone but feeling no pain: Effects of social exclusion on physical pain tolerance and pain threshold, affective forecasting, and interpersonal empathy. Journal of Personality and Social Psychology, 91(1), 1–15. 10.1037/0022-3514.91.1.1 [PubMed: 16834476]

DuPre E, Luh W-M, & Spreng RN (2016). Multi-echo fMRI replication sample of autobiographical memory, prospection and theory of mind reasoning tasks. Scientific Data, 3(October), 160116 10.1038/sdata.2016.116 [PubMed: 27996964]

Fisher G, & Rangel A (2014). Symmetry in cold-to-hot and hot-to-cold valuation gaps. Psychological Science, 25(1), 120–127. 10.1177/0956797613502362 [PubMed: 24220624]

Geib BR, Stanley ML, Wing E. a., Laurienti PJ, & Cabeza R (2017). Hippocampal contributions to the large-scale episodic memory network predict vivid visual memories. Cerebral Cortex (New York, N.Y. : 1991), 27(1), 680–693. 10.1093/cercor/bhv272

Gilbert D (2006). Stumbling on happiness. New York, NY, US: Alfred A. Knopf.

Gilbert DT, & Wilson TD (2007). Prospection: Experiencing the future. Science, 317(5843), 1351–4. 10.1126/science.1144161 [PubMed: 17823345]

Hare T. a, Camerer CF, & Rangel A (2009). Self-control in decision-making involves modulation of the vmPFC valuation system, 324, 646–648.

Hare T. a, Malmaud J, & Rangel A (2011). Focusing attention on the health aspects of foods changes value signals in vmPFC and improves dietary choice. Journal of Neuroscience, 31(30), 11077–87. 10.1523/JNEUROSCI.6383-10.2011 [PubMed: 21795556]

Hutcherson CA, Plassmann H, Gross JJ, & Rangel A (2012). Cognitive regulation during decision making shifts behavioral control between ventromedial and dorsolateral prefrontal value systems. Journal of Neuroscience, 32(39), 13543–13554. 10.1523/JNEUROSCI.6387-11.2012 [PubMed: 23015444]

Jenkinson M, Beckmann CF, Behrens TEJ, Woolrich MW, & Smith SM (2012). FSL. NeuroImage, 62(2), 782–790. 10.1016/j.neuroimage.2011.09.015 [PubMed: 21979382]

Jing HG, Madore KP, & Schacter DL (2016). Worrying about the future: An episodic specificity induction impacts problem solving, reappraisal, and well-being, 145(4), 402–418. Retrieved from 10.1037/xge0000142.supp

Johansen-Berg H, & Rushworth MFS (2009). Using diffusion imaging to study human connectional anatomy. Annual Review of Neuroscience, 32(1), 75–94. 10.1146/annurev.neuro.051508.135735

Kable JW, & Glimcher PW (2007). The neural correlates of subjective value during intertemporal choice. Nature Neuroscience, 10(12), 1625–1633.10.1038/nn2007 [PubMed: 17982449]

Kleiner M, Brainard D, & Pelli D (2007). "What's new in Psychtoolbox-3?" Perception. 36 ECVP Abstract Supplement.

Kundu P, Brenowitz ND, Voon V, Worbe Y, Vertes PE, Inati SJ, … Bullmore ET (2013). Integrated strategy for improving functional connectivity mapping using multiecho fMRI. Proceedings of the National Academy of Sciences of the Unites States of America, 110(40), 16187–16192. 10.1073/pnas.1301725110

Kundu P, Santin MD, Bandettini P. a., Bullmore ET, & Petiet A (2014). Differentiating BOLD and non-BOLD signals in fMRI time series from anesthetized rats using multi-echo EPI at 11.7T. NeuroImage, 102(P2), 861–874. 10.1016/j.neuroimage.2014.07.025 [PubMed: 25064668]

Levy DJ, & Glimcher PW (2011). Comparing apples and oranges: Using reward-specific and reward-general subjective value representation in the brain. Journal of Neuroscience, 31(41), 14693–14707. 10.1523/JNEUROSCI.2218-11.2011 [PubMed: 21994386]

Litt A, Plassmann H, Shiv B, & Rangel A (2011). Dissociating valuation and saliency signals during decision-making. Cerebral Cortex, 21(1), 95–102. 10.1093/cercor/bhq065 [PubMed: 20444840]

Loewenstein G, O'Donoghue T, & Rabin M (2003). Projection bias in predicting future utility. The Quarterly Journal of Economics, 118(4), 1209–1248.

Loewenstein G (1996). Out of control: Visceral influences on behavior. Organizational Behavior and Human Decision Processes, 65(3), 272–292.

Lombardo MV, Auyeung B, Holt R, Waldman J, Ruigrok A, Mooney N, … Kundu P (2015). Improving effect size and power with multi-echo fMRI and its impact on understanding the neural systems supporting mentalizing.

Menon V, & Uddin LQ (2010). Saliency, switching, attention and control: a network model of insula function. Brain Struct Funct, 214(5–6), 655–667. 10.1007/s00429-010-0262-0.Saliency [PubMed: 20512370]

Mitchell AS (2015). The mediodorsal thalamus as a higher order thalamic relay nucleus important for learning and decision-making. Neuroscience and Biobehavioral Reviews, 54, 76–88. 10.1016/j.neubiorev.2015.03.001 [PubMed: 25757689]

Nakamura K, & Hikosaka O (2006). Role of dopamine in the primate caudate nucleus in reward modulation of saccades. Journal of Neuroscience, 26(20), 5360–5369. 10.1523/JNEUROSCI.4853-05.2006 [PubMed: 16707788]

Okuda J, Fujii T, Yamadori A, Kawashima R, Tsukiura T, Fukatsu R, … Fukuda H (1998). Participation of the prefrontal cortices in prospective memory: Evidence from a PET tudy in humans. Neuroscience Letters, 253(2), 127–130. 10.1016/S0304-3940(98)00628-4 [PubMed: 9774166]

Pelli DG (1997) The VideoToolbox software for visual psychophysics: Transforming numbers into movies, Spatial Vision 10:437–442. [PubMed: 9176953]

Peters J, & Buchel C (2010). Episodic future thinking reduces reward delay discounting through an enhancement of prefrontal-mediotemporal interactions. Neuron, 66(1), 138–148. 10.1016/j.neuron.2010.03.026 [PubMed: 20399735]

Plassmann H, & Weber B (2015). Individual differences in marketing placebo effects: Evidence from brain imaging and behavioral experiments. Journal of Marketing Research, 52(4), 493–510. 10.1509/jmr.13.0613

Plassmann H, O'Doherty J, & Rangel a. (2007). Orbitofrontal cortex encodes willingness to pay in everyday economic transactions. Journal of Neuroscience, 27(37), 9984–9988. 10.1523/JNEUROSCI.2131-07.2007 [PubMed: 17855612]

Read D, & van Leeuwen B (1998). Predicting hunger: The effects of appetite and delay on choice. Organizational Behavior and Human Decision Processes, 76, 189–205. [PubMed: 9831521]

Reisberg D, Smith JD, Baxter DA, & Sonenshine M (1989). "Enacted" auditory images are ambiguous; "Pure" auditory images are not. The Quarterly Journal of Experimental Psychology Section A, 41(3), 619–641. 10.1080/14640748908402385

Samanez-Larkin GR, & Knutson B (2015). Decision making in the ageing brain: changes in affective and motivational circuits. Nature Reviews Neuroscience, 16(5), 278–289. 10.1038/nrn3917 [PubMed: 25873038]

Schacter DL (2012). Adaptive constructive processes and the future of m emory. American Psychologist, 603–613. 10.1038/nn1252 [PubMed: 23163437]

Schacter DL, Addis DR (2009). On the nature of medial temporal lobe contributions to the constructive simulation of future events. Philosophical Transactions of the Royal Society, 1245–1253. 10.1098/rstb.2008.0308

Schultz W (2000). Multiple reward signals in the brain. Nature Reviews, 1(9), 199–207. 10.1038/35044563

Shohamy D, & Adcock RA (2010). Dopamine and adaptive memory. Trends in Cognitive Sciences, 14(10), 464–472. 10.1016/j.tics.2010.08.002 [PubMed: 20829095]

Spreng RN, Gerlach KD, Turner GR, & Schacter DL (2015). Autobiographical planning and the brain: Activation and its modulation by qualitative features. Journal of Cognitive Neuroscience. 10.1162/jocn

Staudinger MR, Erk S, & Walter H (2011). Dorsolateral prefrontal cortex modulates striatal reward encoding during reappraisal of reward anticipation. Cerebral Cortex, 21(11), 2578–2588. 10.1093/cercor/bhr041 [PubMed: 21459835]

Swenson R (2006). Chapter 10-Thalamic Organization. In Review of Clinical and Functional Neuroscience. Retrieved from https://www.dartmouth.edu/~rswenson/NeuroSci/index.html

Trope Y, & Liberman N (2010). Construal-level theory of psychological distance. Psychological Review, 117(2), 440–63. 10.1037/a0018963 [PubMed: 20438233]

Van Essen DC (2005). A population-average, landmark- and surface-based (PALS) atlas of human cerebral cortex. NeuroIma, 28, 635–662.

Vincent JL, Kahn I, Snyder a. Z., Raichle ME, & Buckner RL (2008). Evidence for a frontoparietal control system revealed by intrinsic functional connectivity. Journal of Neurophysiology, 100(6), 3328–3342. 10.1152/jn.90355.2008 [PubMed: 18799601]

Waskom ML, Kumaran D, Gordon a. M., Rissman J, & Wagner a. D. (2014). Frontoparietal representations of task context support the flexible control of goal-directed cognition. Journal of Neuroscience, 34(32), 10743–10755. 10.1523/JNEUROSCI.5282-13.2014 [PubMed: 25100605]

Wimmer GE, & Shohamy D (2012). Preference by association: How memory mechanisms in the hippocampus bias decisions. Science, 338, 270–273. 10.1126/science.1223252 [PubMed: 23066083]

Wolosin SM, Zeithamova D, & Preston AR (2012). Reward modulation of hippocampal subfield activation during successful associative encoding and retrieval. Journal of Cognitive Neuroscience, 24(7), 1532–1547. 10.1162/jocn_a_00237 [PubMed: 22524296]

Yarkoni T, Poldrack RA, Nichols TE, Essen DC Van, Tor D, & Group WM (2012). Large-scale automated synthesis of human functional neuroimaging data. Nature Methods, 8(8), 665–670. 10.1038/nmeth.1635.Large-scale

Yeo TBT, Krienen FM, Sepulcre J, Sabuncu MR, Lashkari D, Hollinshead M, … Buckner RL (2011). The organization of the human cerebral cortex estimated by intrinsic functional connectivity. Journal of Neurophysiology, 106(3), 1125–1165. http://doi.org/10.n52/jn.00338.2011 [PubMed: 21653723]

Highlights:

- Individuals miscalculate value of food items in dissimilar future context (bias)

- Imagination of similar context to the present involves caudate and hippocampus

- Imagination of dissimilar context related to regions involved in cognitive control

- Bias positively related to brain activity in ventral striatum

- Bias negatively related to brain activity in thalamus and posterior insula
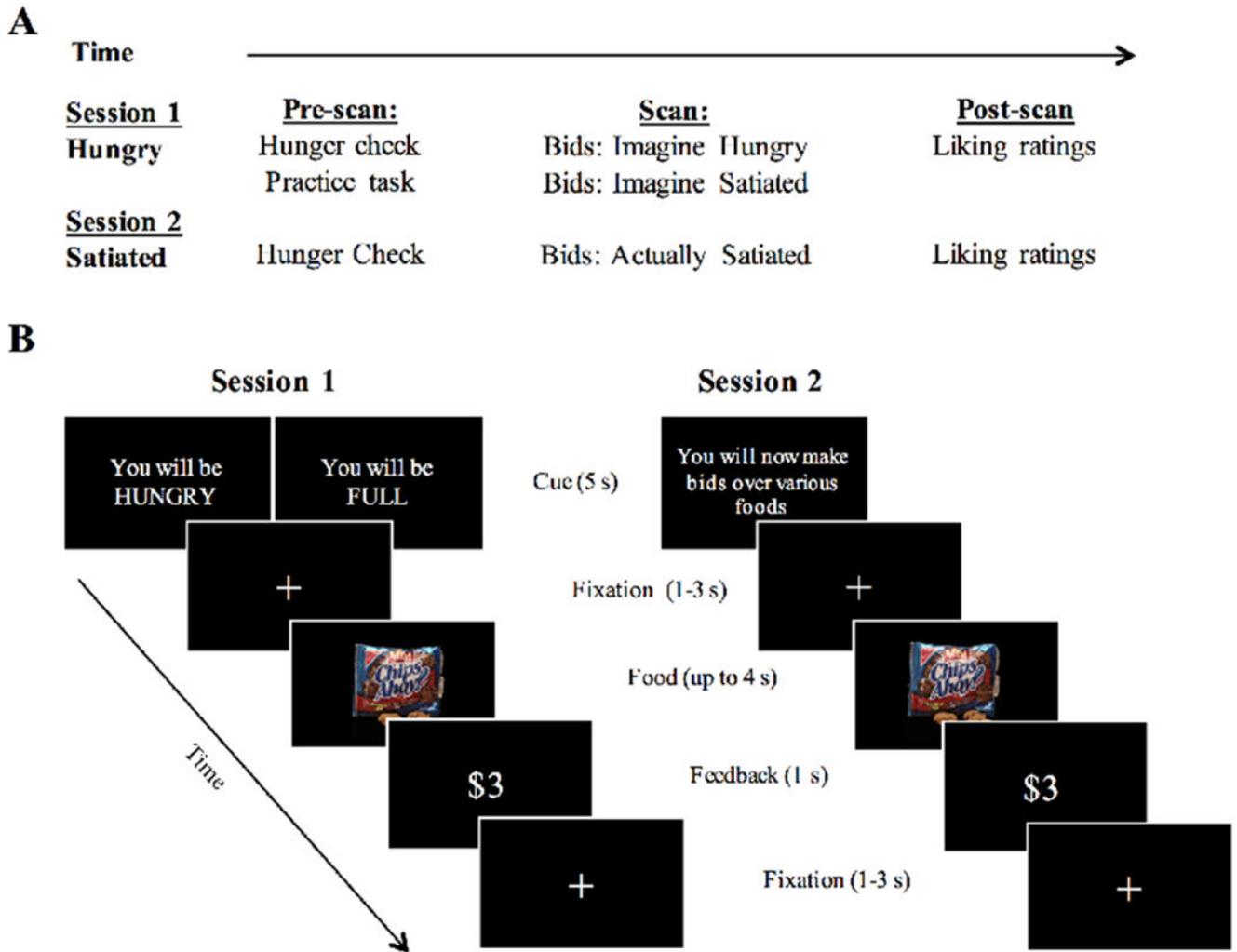
Figure 1. Experimental Procedure.
A, The timeline of study activities over two scanning sessions. *B*, The left panel illustrates the onset of a block from session one, where the block instructions serve as a cue for which condition will follow. Identical stimuli were used for Imagine Hungry and Imagine Satiated, but presentation of the food items was randomized. Block presentation was also randomized but constrained to a maximum of two of the same blocks back-to-back. The right panel shows the onset of a block during the second scanning session. The same 90 food images were used as in the first scanning session, but only appeared once. Presentation of food items was again randomized for each participant.
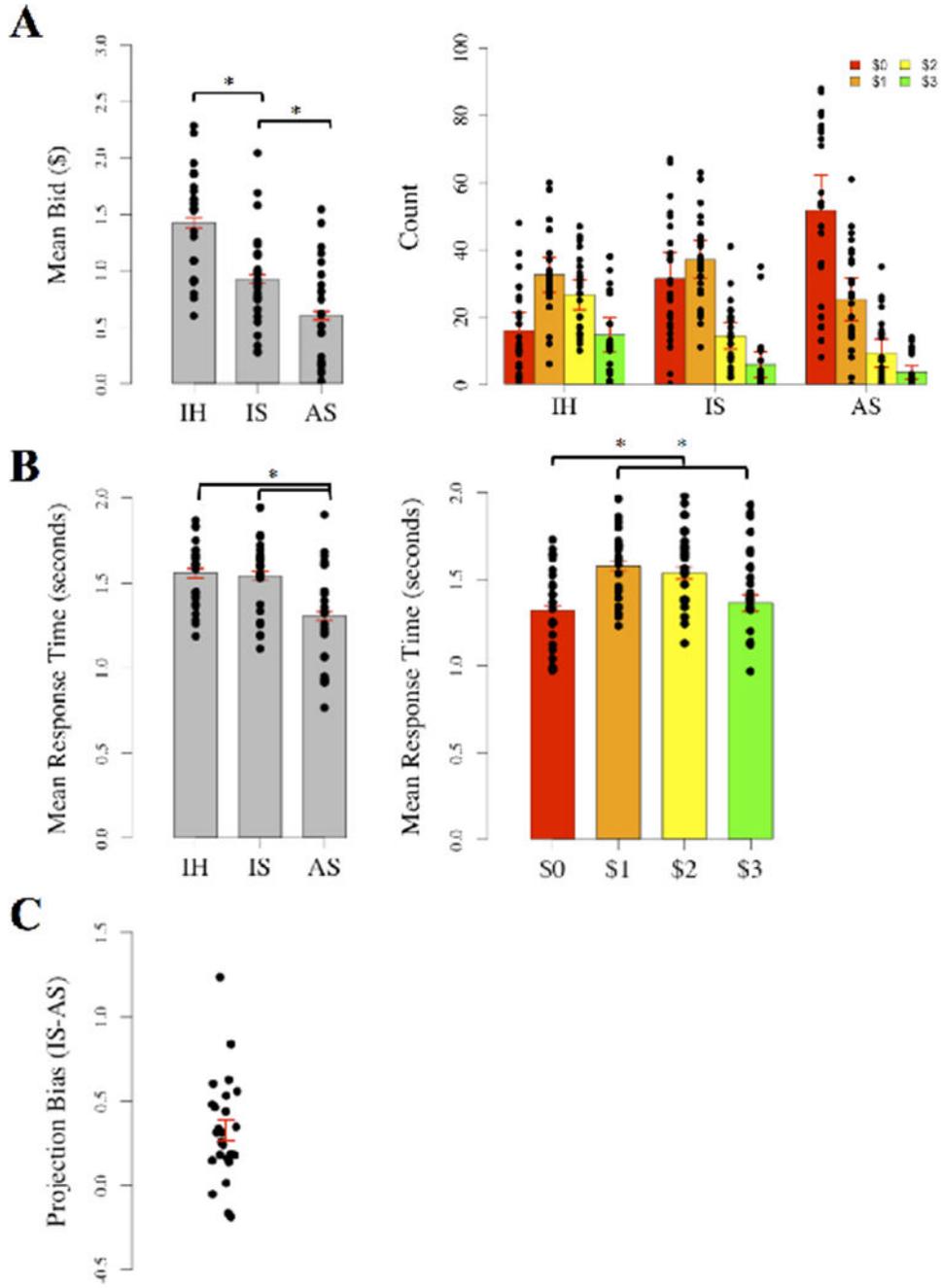
Figure 2. Behavioral Results.

A, Bar graphs illustrating how mean bids and the pattern of different bid amounts varied across conditions (See Table S1 for full list of significant pairwise differences from right panel). *B*, Bar graphs illustrating RT differences across conditions and by bid amount. *C*, Distribution of projection bias scores. Dots in each plot represent the mean for each participant. Standard error bars indicate 1 standard error around the mean. * denotes pairwise differences of $p<.0001$. *IH* = Imagine Hungry, *IS* = Imagine Satiated, *AS* = Actually Satiated.
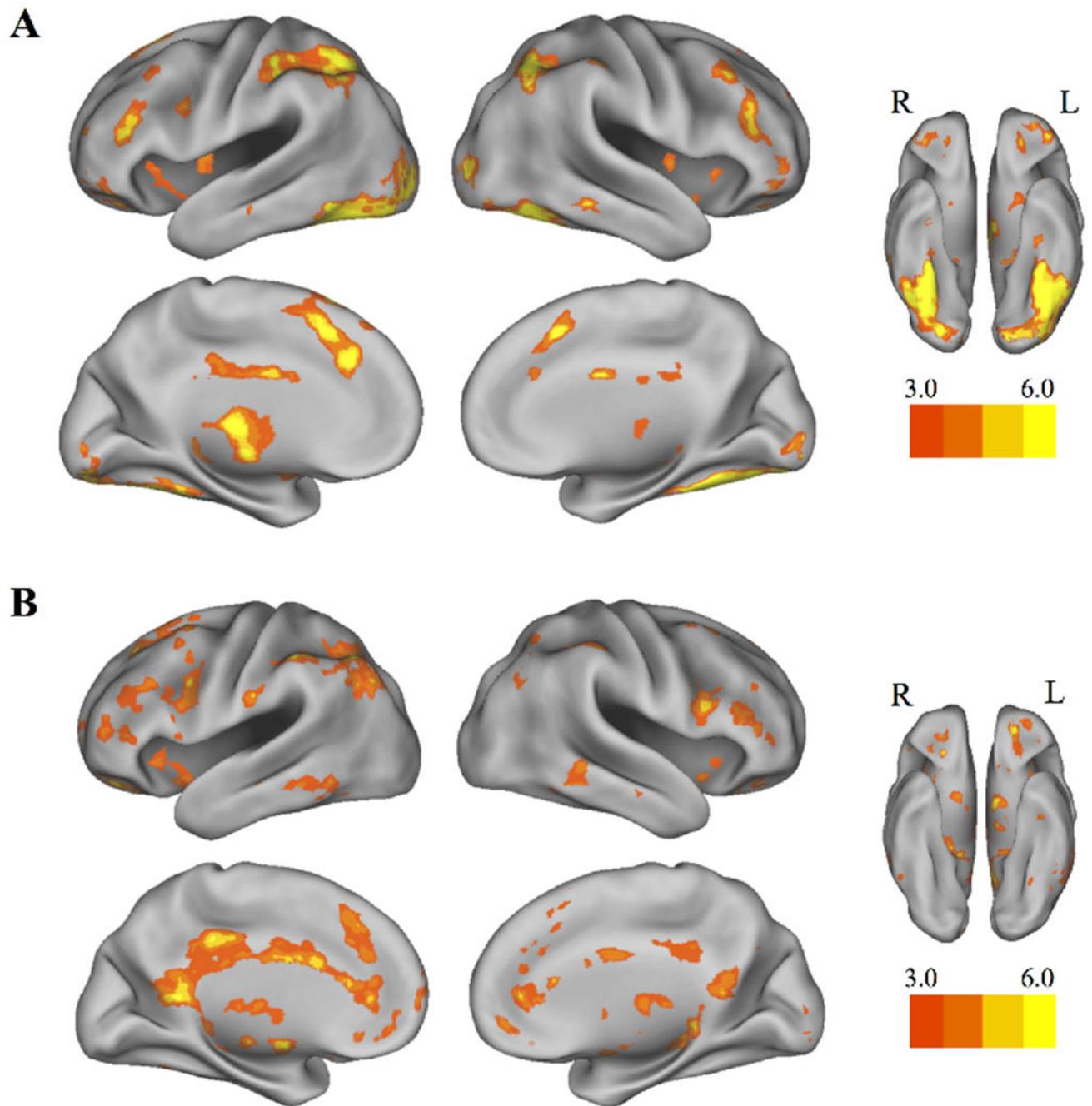
Figure 3. Overall activation during the bidding task.
Collapsed across task conditions from both scanning sessions, *A*, whole-brain activation for the bidding task and *B*, for parametric modulation of bid amount (GLM1). Results were thresholded at $p<.001$ (uncorrected), k=20. Colorbars denote t values, lowered to t=3 for visualization purposes.
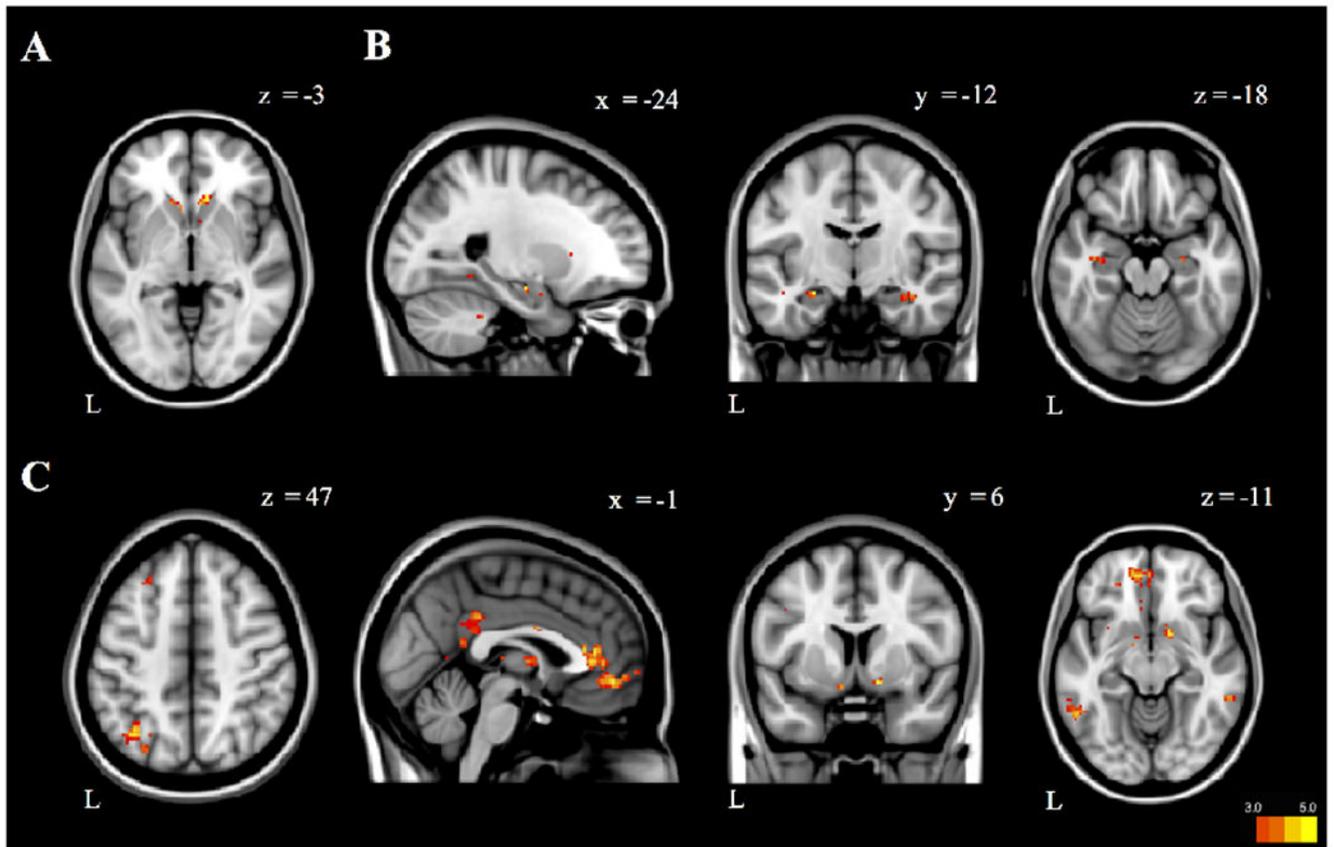
Figure 4. Influence of congruent context on future valuation.
A-B, Parametric modulation of bids during Imagine Hungry > Imagine Satiated (GLM1) compared to *C*, high- versus low-value trials during Imagine Hungry alone (GLM3). Results were thresholded at $p<.001$ (uncorrected), k=10. Colorbars denote t values, lowered to t=3 for visualization purposes.
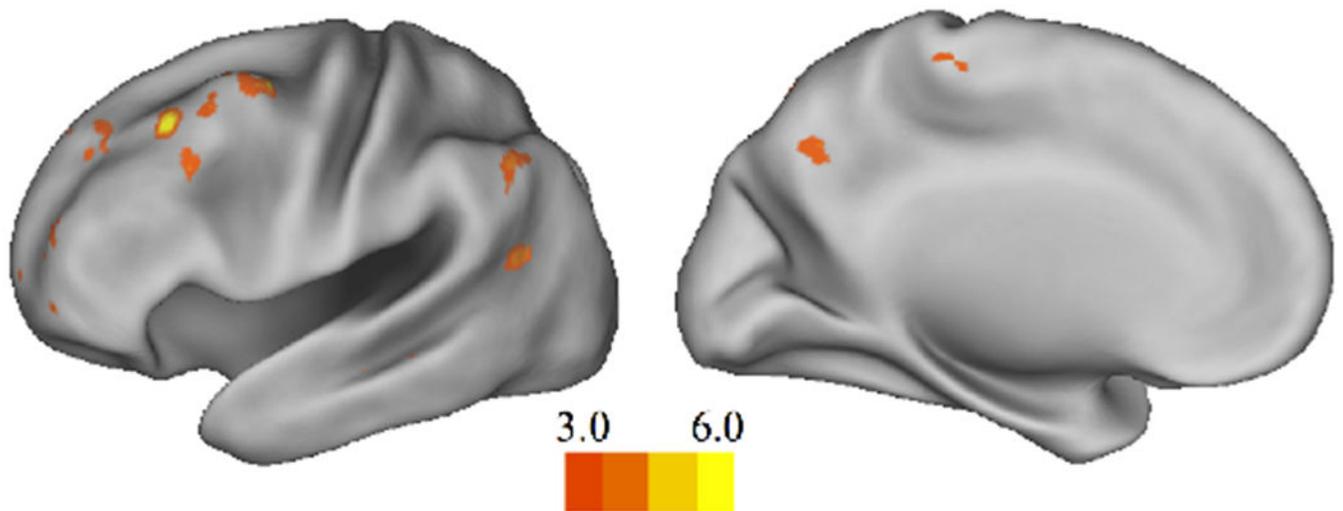
Figure 5. Influence of incongruent context on future valuation.
Whole-brain activation during Imagine Satiated > Imagine Hungry (GLM1). Results were thresholded at $p<.001$ (uncorrected), k=10. Colorbars denote t values, lowered to t=3 for visualization purposes.
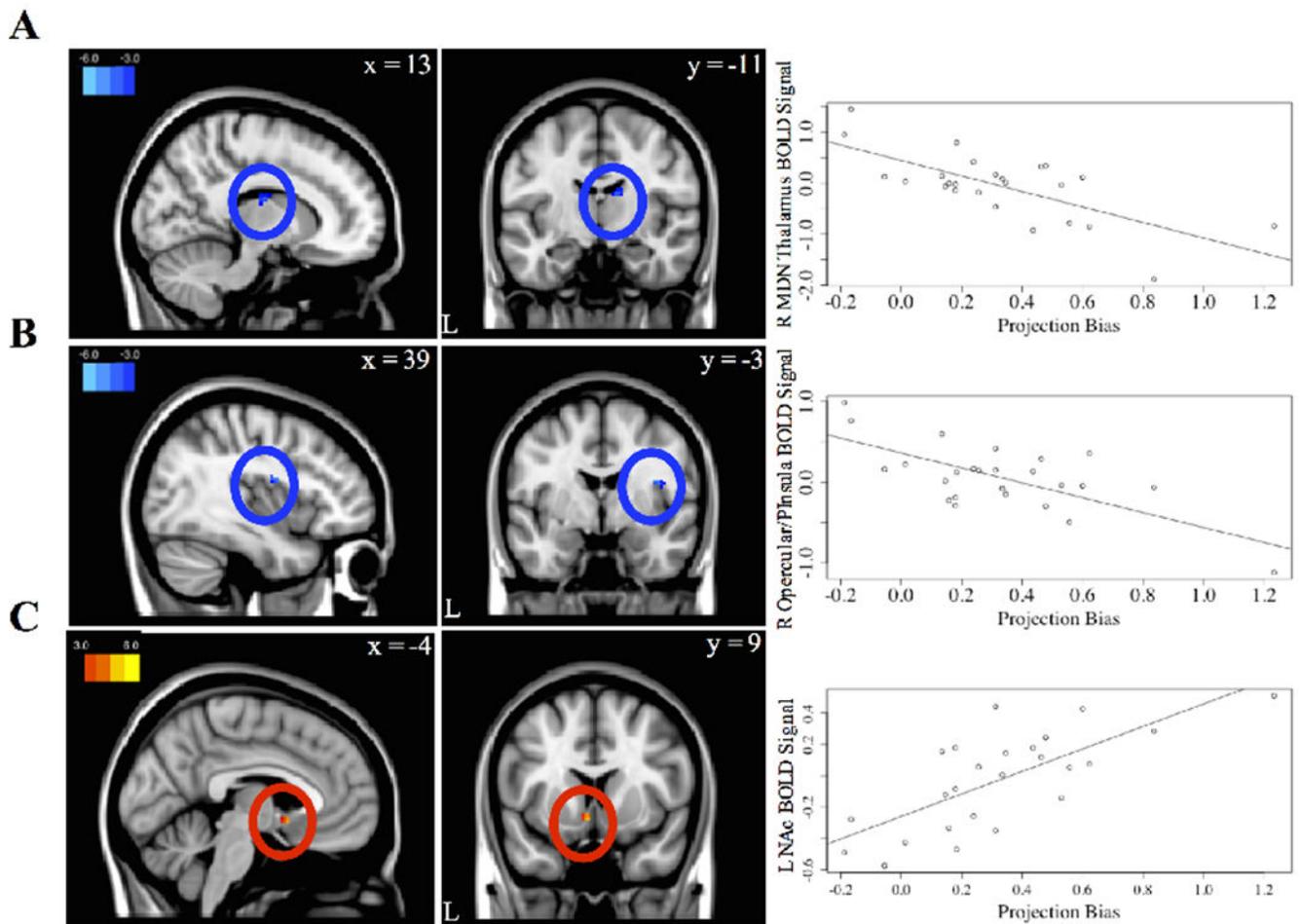
Figure 6. Brain activation during incongruent motivational context related to projection bias.
BOLD signal in *A*, the right medial dorsal nucleus (MDN) of the thalamus, *B*, right opercular cortex/posterior insula, and *C*, left nucleus accumbens are associated with projection bias scores (GLM2). Projection bias scores were calculated as the mean bid in Imagine Satiated minus the mean bid in Actually Satiated. Projection bias scores were then entered as a regressor at the second level into GLM2, the model without parametric modulation. Results were thresholded at $p<.001$ (uncorrected), k=10. Beta weights from the identified clusters (left panel) were extracted and plotted against projection bias scores (right panel) for illustration only. Colorbars denote t values, lowered to t=|3| for visualization purposes.

Table 1:

Areas showing activation collapsed across conditions from both days of the bidding task (GLM1).

Region	Laterality	Voxels	MNI coordinates			t	z	
			x	y	z			
Superior Parietal Lobe	L	1819	−46	−42	54	9.98	6.22	*
Temporal Occipital Fusiform Cortex	L	8686	−38	−64	−16	9.94	6.2	*
Paracingulate Gyrus/Superior Frontal Gyrus	L	1281	−2	18	46	8.56	5.74	*
Frontal Pole/Lateral Orbitofrontal cortex	L	76	−24	38	−18	8.36	5.67	*
Thalamus	L	1799	−10	−20	10	7.97	5.52	*
Superior Lateral Occipital Cortex/Angular Gyrus	R	856	42	−58	46	7.83	5.47	*
Caudate	R	287	16	16	2	7.71	5.42	*
Insular Cortex	L	107	−40	−4	10	6.86	5.06	*
Frontal Pole	L	148	−40	42	−14	6.21	4.75	*
Dorsal Anterior Cingulate Gyrus	R	24	6	−2	28	6.12	4.7	
Hippocampus	R	145	24	−32	0	5.98	4.63	*
Middle Frontal Gyrus	R	281	50	32	22	5.98	4.63	*
Inferior Frontal Gyrus/Dorsolateral Prefrontal Cortex	R	313	42	30	16	5.96	4.62	*
Middle Frontal Gyrus	R	102	44	24	40	5.49	4.38	*
Dorsal Anterior Cingulate Gyrus	L	170	−4	−6	28	5.32	4.28	*
Anterior Parahippocampal Gyrus	L	21	−30	−8	−32	5.21	4.22	
Supramarginal Gyrus	R	139	52	−32	48	5.14	4.18	*
Frontal Pole	R	20	22	42	−20	5.1	4.16	
Cerebellum		54	0	−50	0	4.99	4.09	
Precentral Gyrus	L	112	−56	10	34	4.98	4.09	*
Middle Frontal Gyrus	L	37	−36	22	40	4.87	4.02	
Frontal Pole/Ventrolateral Prefrontal Cortex	R	87	38	42	−14	4.85	4.01	*
Temporal Fusiform Cortex	L	30	−34	−24	−24	4.61	3.87	
Frontal Pole	R	41	42	48	−2	4.61	3.86	
Frontal Pole	L	44	−8	42	48	4.22	3.61	
Putamen	R	34	26	4	0	4.2	3.6	

Height threshold: t(24)=3.47, p<.001 (uncorrected); extent threshold, k=20. L=Left, R=Right.

*
Survives FWE correction at p<.05.

Table 2:

Areas showing parametric modulation of bids collapsed across task conditions from both days of the bidding task (GLM1).

Region	Laterality	Voxels	MNI coordinates			t	z	
			x	y	z			
Frontal Pole/Ventrolateral Prefrontal Cortex	L	257	−22	46	−18	7.32	5.25	*
Supramarginal Gyrus	L	1222	−46	−42	48	6.82	5.04	*
Posterior Cingulate Cortex/Retrosplenial Cortex	L	1773	−4	−50	10	6.58	4.93	*
Middle Frontal Gyrus	L	677	−28	16	58	6.39	484	*
Pallidum	L	232	−10	−2	−6	6.29	4.79	*
Inferior Temporal Gyrus	L	341	−52	−30	−18	5.94	4.61	*
Insular Cortex	L	82	−40	12	−12	5.91	4.6	*
Postcentral Gyrus	L	61	−56	−20	26	5.86	4.57	
Middle Frontal Gyrus	L	530	−48	20	32	5.82	4.55	*
Temporal Pole	R	46	44	10	−14	5.81	4.55	
Orbitofrontal Cortex	R	25	24	28	−20	5.7	4.49	
Hippocampus	R	111	26	−26	−4	5.56	4.41	*
Cerebellum	R	36	2	−60	−30	5.42	4.34	
Frontal Pole/Orbitofrontal Cortex	R	74	26	36	−18	5.32	4.28	
Rostrolateral Prefrontal Cortex	R	242	48	38	22	5.31	4.28	*
Thalamus	L	197	−12	−16	0	5.18	4.2	*
Inferior Frontal Gyrus/Dorsolateral Prefrontal Cortex	R	204	50	14	18	5.17	4.2	*
Cerebellum	R	134	20	−50	−24	5.02	4.11	*
Cerebellum	R	38	12	−72	−22	4.98	4.09	
Ventral Striatum/Nucleus Accumbens	R	87	12	4	4	4.97	4.08	*
Putamen	L	101	−30	−4	0	4.97	4.08	*
Supramarginal Gyrus	R	154	40	−42	42	4.96	4.07	*
Cerebellum	R	81	4	−54	−50	4.94	4.06	*
Paracingulate Gyrus/Superior Frontal Gyrus/Dorsal Anterior Cingulate Cortex	L	249	−4	30	38	4.92	4.05	*
Thalamus	R	58	10	−14	12	4.77	3.96	
Inferior Temporal Gyrus	R	152	54	−44	−16	4.73	3.93	*
Middle Frontal Gyrus	R	7	32	16	54	4.72	3.93	
Temporal Occipital Fusiform Cortex	L	20	−28	−56	−20	4.61	3.86	
Cerebellum	R	27	14	−68	−46	4.6	3.86	
Cerebellum	R	73	44	−64	−46	4.58	3.85	
Anterior Cingulate Gyrus	R	39	8	−2	30	4.58	3.85	
Orbitofrontal Cortex	L	21	−14	14	−20	4.54	3.82	
Frontal Pole	L	33	−6	64	2	4.36	3.71	
Cerebellum	L	112	−44	−56	−46	4.36	3.7	*
Insular Cortex	L	27	−32	20	−4	4.32	3.68	
Superior Parietal Lobe	R	38	34	−56	54	4.28	3.65	
Caudate	L	20	−16	−2	18	4.28	3.65	

Region	Laterality	Voxels	MNI coordinates			*t*	*z*
			x	**y**	**z**		
Cerebellum	L	20	−8	−72	−26	4.21	3.61
Lateral Occipital Cortex	R	49	36	−58	44	4.17	3.58
Frontal Pole	L	31	−24	54	10	4.16	3.57
Brainstem		44	0	−30	−30	4.16	3.57
Cerebellum	R	20	28	−70	−26	4.06	3.51
Caudate	L	20	−8	14	6	3.95	3.43

Height threshold: t(24)=3.47, p<.001 (uncorrected); extent threshold, k=20. L=Left, R=Right.

*
Survives FWE correction at p<.05.

Table 3:

Areas showing parametric modulation of bids during Imagine Hungry > Imagine Satiated (GLM1).

Region	Laterality	Voxels	MNI coordinates			t	z
			x	y	z		
Caudate	R	29	12	24	−2	5.17	4.2
Temporal Fusiform Cortex	R	10	42	−32	−10	5.11	4.16
Caudate	L	25	−6	20	0	4.77	3.96
Hippocampus	R	18	38	−10	−18	4.37	3.71
Brainstem	R	15	6	−46	−52	4.24	3.63
Subcallosal Cortex		19	0	10	4	4.12	3.55
Hippocampus	L	19	−42	−16	−12	4.05	3.5
Lateral Occipital Cortex	L	11	−20	−68	−36	3.99	3.46
Cerebellum	L	11	−16	−36	−32	3.87	3.38

Height threshold: t(24)=3.47, p<.001 (uncorrected); extent threshold, k=10. L=Left, R=Right.

Table 4:

Areas showing High > Low activation during Imagine Hungry (GLM3).

Region	Laterality	Voxels	MNI coordinates			t	z	
			x	y	z			
Middle Frontal Gyrus	L	67	−28	16	56	6.77	5.01	*
Putamen	R	12	14	6	−10	6.23	4.76	
Subcallosal Cortex	L	38	−6	22	−4	5.53	4.4	
Superior Frontal Gyrus	L	87	−20	22	40	5.19	4.21	*
Middle Cingulate Cortex	L	39	−4	−6	28	5.18	4.2	
Anterior Cingulate Cortex	R	99	2	34	6	5.11	4.16	*
Posterior Cingulate Cortex	L	140	−4	−38	34	5.1	4.16	*
Frontal Pole	L	12	−12	66	18	4.93	4.06	
Medial Prefrontal Cortex		168	0	48	−6	4.89	4.03	*
Angular Gyrus	L	203	−32	−60	46	4.88	4.03	*
Precuneus	L	136	−6	−58	20	4.8	3.98	*
Frontal Pole	L	29	−22	44	−16	4.79	3.98	
Nucleus Accumbens	L	20	−10	10	−12	4.69	3.91	
Inferior Temporal Gyrus	L	91	−54	−52	−10	4.67	3.9	*
Thalamus	L	27	−6	−4	8	4.61	3.86	
Cerebellum	R	33	40	−70	−42	4.59	3.85	
Temporal Occipital Fusiform Cortex	R	10	22	−42	−20	4.38	3.72	
Cerebellum	L	10	−22	−76	−42	4.36	3.7	
Middle Temporal Gyrus	R	21	58	−40	−10	4.34	3.69	
Middle Temporal Gyrus	R	10	50	−18	−18	4.29	3.66	
Brain Stem	R	20	10	−48	−40	4.28	3.65	
Thalamus	L	11	−10	−10	14	4.26	3.64	
Temporal Occipital Fusiform Cortex	R	12	48	−58	−24	4.24	3.63	
Brainstem	L	10	−4	−52	−48	4.21	3.6	
Anterior Cingulate Cortex	L	15	−2	12	24	4.14	3.56	
Inferior Frontal Gyrus	L	10	−48	12	26	3.88	3.39	

Height threshold: t(24)=3.47, p<.001 (uncorrected); extent threshold, k=10. L=Left, R=Right.

*
Survives FWE correction at p<.05.

Table 5:

Areas showing activation during Imagine Satiated > Imagine Hungry (GLM2).

Region	Laterality	Voxels	MNI coordinates			t	z	
			x	y	z			
Middle Frontal Gyrus	L	90	−34	24	44	6.44	4.86	*
Frontal Pole	L	50	−24	64	2	5.62	4.45	
Cerebellum	R	60	24	−84	−34	5.5	4.38	
Middle Frontal Gyrus	L	50	−34	0	54	5.09	4.15	
Inferior Temporal Gyrus	L	21	−50	−18	−22	4.83	4	
Angular Gyrus	L	41	−50	−56	44	4.83	3.99	
Precuneus	L	31	−2	−60	40	4.68	3.9	
Frontal Pole	L	25	−34	54	24	4.62	3.87	
Angular Gyrus	R	23	58	−52	28	4.59	3.85	
Angular Gyrus	L	36	−44	−60	18	4.38	3.72	
Middle Frontal Gyrus	L	24	−38	20	34	4.29	3.66	
Postcentral Gyrus	R	52	4	−38	74	4.14	3.56	
Frontal Pole	L	30	−22	38	44	4.12	3.55	

Height threshold: t(24)=3.47, p<.001 (uncorrected); extent threshold, k=20. L=Left, R=Right.

*
Survives FWE correction at p<.05.

Table 6:

Areas showing a relationship with projection bias scores (GLM2).

Direction	Region	Laterality	Voxels	MNI coordinates			t	Z
				x	y	z		
-	Thalamus (dorsomedial nucleus)	R	22	12	−14	18	5.09	4.12
-	Opercular Cortex/Posterior Insula	R	19	42	−6	22	4.69	3.89
+	Ventral Striatum/Nucleus Accumbens	L	10	−2	10	−8	5.14	4.15

Height threshold: t(24)=3.48, p<.001 (uncorrected); extent threshold, k=10. L=Left, R=Right.